Journal of Geomine (2025), 3(3), 155-164
DOI: 10.22077/jgm.2025.10207.1060

Geostatistical assessment of ore reserve estimation accuracy in the Hired Gold Deposit

Komei Kaheni[1], Ahmad Reza Mokhtari[1], Hadi Farhadian[2]

Recived: 2025 Oct. 05, Revised: 2025 Nov. 22, Accepted: 2025 Nov. 23, Published: 2025 Dec. 12

ABSTRACT

Accurate ore reserve estimation is essential for effective mine planning, particularly in deposits with highly skewed grade distributions, such as gold. This study focuses on the Hired gold deposit (Anomaly 3), located south of Birjand, where 1,583 trench and borehole samples were composited into 2,124 data points for geostatistical analysis. Three estimation techniques—Ordinary Kriging (OK), Full Indicator Kriging (FIK), and Sequential Gaussian Simulation (SGS)—were employed to model grade distribution and estimate ore tonnage. Data normalization, variogram modeling, and block modeling were performed to construct three-dimensional representations of the deposit. Model accuracy and reliability were evaluated using grade–tonnage curves and cross-validation analyses. The results indicate that FIK provides more robust estimates than OK and SGS, closely reflecting the actual grade distribution while minimizing the impact of high-grade outliers. At a cut-off grade of 0.1 g/t, the deposit contains an estimated 3.42 Mt of ore with an average grade of 0.75 g/t. Overall, the study demonstrates the effectiveness of FIK for resource estimation in gold deposits characterized by pronounced grade variability and skewed statistical distributions.

KEYWORDS

Geostatistics, Hired Gold Deposit, Resource Estimation, Indicator Kriging, Ordinary Kriging, Sequential Gaussian Simulation

I. INTRODUCTION

After confirming the presence of an economically viable deposit through exploration, estimating the spatial distribution of grade becomes essential for reserve calculation and mine planning (Nejad Hosseini Fashkhami, 2009). Since sampling typically covers only a small portion of the deposit, grades in unsampled areas must be predicted, which is challenging due to geological complexity and lithological variations. Various estimation methods have been developed for this purpose, ranging from simple deterministic approaches such as inverse distance weighting (IDW) and polygonal methods to geostatistical techniques like kriging, each with its own advantages and limitations (Dominy et al., 2002; Aryafar et al., 2020; Daya, 2012; Daya, 2014; Daya and Zaremotlagh, 2013; Ghahremani, 2017; Aryafar & Moeini, 2017).

In gold deposits, reserve estimation is particularly complex because grade distributions are typically highly skewed and strongly influenced by extreme high-grade values (Hasani Pak & Sharafedin, 2001; Kapageridis, 1999; Saed & Farhadian, 2025). These outliers affect statistical parameters, variogram modeling, and ultimately the quality of predictions. Several strategies exist to address this challenge, including data transformation, separate treatment of extreme values, and the use of non-parametric approaches (Aryafar & Roshanravan, 2020; Saito & Goovaerts, 2000; Farhadian & Nikvar-Hassani, 2020; Shademan & Farhadian, 2023; Dehshibi et al., 2022; Aryafar & Roshanravan, 2021).

Among these methods, indicator kriging (IK) has been widely applied in mineral resource estimation. IK does not assume normality, preserves grade variability, and provides probabilistic estimates of ore distribution (Journel, 1986; Kyriakidis & Journel, 1999; Goovaerts, 1997; Lin et al., 2002; Daya, 2015). Numerous studies have confirmed its suitability for deposits with complex grade distributions, including gold (Abzalov & Humphreys, 2002; Rossi & Deutsch, 2013; Alhassan et al., 2015; Rahimi et al., 2016).

Nevertheless, no single estimator universally outperforms the others; the choice depends on deposit characteristics and project objectives (Parker, 1991; Chanderman et al., 2017; Farhadian & Maleki, 2023). Therefore, a comparative assessment of alternative methods is necessary to select the most appropriate approach.

This study applies three geostatistical techniques—Ordinary Kriging (OK), Full Indicator Kriging (FIK), and

[1]Department of Mining Engineering, Isfahan University of Technology, Isfahan 84156-83111, Iran, [2]Department of Mining Engineering, Faculty of Engineering, University of Birjand, Birjand, Iran
✉ H. Farhadian: farhadian@birjand.ac.ir

Sequential Gaussian Simulation (SGS)—to the Hired gold deposit. By evaluating their performance, the research identifies the most reliable method for capturing grade variability and quantifying local uncertainty, thereby improving the accuracy of resource estimation and supporting subsequent mine design.

II. Location and Geographical Conditions

The Hired gold mineralization is located 160 km south of Birjand and 80 km north of Nehbandan (Fig. 1). This area is covered by the geological maps of Dehsalm (scale 1:25,000) and Basiran (scale 1:100,000). The Hired Gold Anomaly No. 3 lies within the geographical coordinates of 704,400 to 706,500 meters east longitude and 3,535,923 to 3,537,723 meters north latitude in the UTM coordinate system. This anomaly (No. 3) is situated approximately 7 km east-southeast of Basiran village. Access to the study area is available via the asphalt road connecting Birjand, Khusf, and Basiran.

A. Geology of the Survey Area

The Heird exploration area, classified within the major sedimentary–structural domains of Iran, is situated in the eastern part of the Central Iran microcontinent. This microcontinent is a subdivision of Central Iran, bounded by the Sistan ophiolitic suture, the Naein–Baft ophiolitic belt, the Doruneh fault, and the Kashmar–Sabzevar ophiolites. It is further divided by long, westward-trending right-lateral strike-slip faults into several tectonic subdomains, including the Lut Block, Shotori Range, Tabas Basin, Kalmard Block, Posht-e-Badam Block, Biyazeh–Bardsir Depression, and the Yazd-Lut Block (Fig. 2).

The Heird mineralized zone is situated along the eastern to northeastern margin of the Lut Block, adjacent to the Flysch Zone of eastern Iran (Samanai & Ashtari, 1992). The majority of the Lut Block consists of Cenozoic volcanic rocks, although sporadic outcrops of Paleozoic and, particularly, Mesozoic sediments are also present. Additionally, parts of the Lut Block are covered by continental, undeformed Plio-Quaternary sediments. Granitoid intrusions of Late Jurassic and Tertiary age have locally intruded and affected the older rocks of the Lut Block. The stratigraphic record of the Lut Block closely resembles that of other domains within the Central Iran microcontinent (Rostamipour et al., 2024). The intrusive bodies within the Heird mineralized zone can be classified into two general groups: (1) Magnetite-series (oxidized) intrusions and (2) Ilmenite-series (reduced) intrusions. Magnetite-series intrusions (Type I) typically form in island-arc and continental margin subduction zones. Their characteristic minerals include magnetite, hornblende, biotite, calcite, and sphene. The magnetite content is approximately 1–2%, with magnetic susceptibility values exceeding 60×10^{-5} SI (Askari et al., 2015). Ilmenite-series intrusions (mostly S-type) are generally associated with continental collision zones. They are mainly granitic in composition, with diagnostic minerals such as biotite, ilmenite, and tourmaline. The ilmenite content in reduced granitoids ranges from 1–5%, and their magnetic susceptibility is less than 60×10-5 SI. Hydrothermal alteration and mineralization in the Heird exploration area are strongly influenced by these intrusive bodies. The dominant lithological units in the study area mainly consist of Eocene volcanics and pyroclastics, which are overlain in the northern and southern parts by Quaternary sediments. The volcanic units comprise altered basaltic andesites, pyroxene andesites, hornblende andesites, andesites, crystal tuffs, and ignimbrites. The propylitized andesites and pyroxene andesites, as well as volcanic lava flows, are extensively altered. Additionally, a hornblende quartz monzonite intrusion occurs in the northern part of the exploration zone (Aghanabati, 2004).

III. Ore Reserve Estimation Using OK, IK, and Sequential Gaussian Simulation

To examine and understand the variability and characteristics of each measured variable, frequency histograms were plotted, and relevant statistical parameters were calculated. Samples with a grade of zero were excluded from the dataset during the statistical analysis. The total number of samples analyzed was 1,583, collected from 63 trenches and 32 boreholes drilled in Anomaly 3 of the Hired Gold Deposit. For these samples, distribution parameters—including mean, variance, and standard deviation—were computed. Specifically, 980 samples were obtained from boreholes, and 603 samples were collected from trenches. The average grade across all samples was 0.71 ppm, with a standard deviation of 2.81 ppm. The skewness and kurtosis values for the gold variable were 11.37 and 179.77, respectively.

A. Regularization and Composite Construction

To assess the reserve using geostatistical methods, it is necessary to define the spatial structure of the distribution of variables. The first step in applying geostatistical methods is to use datasets with consistent bases, where the sampling population forms a homogeneous and equiprobable environment in terms of the volume or length of the collected samples. Ideally, all samples should be collected under identical conditions regarding sample length and dimensions. When samples vary in size and volume, they must be standardized to a common base using numerical methods. For the samples collected from this deposit, it is assumed that all sampling conditions, except for sample length, are consistent. Using a weighted average based on sample length, all samples collected along a borehole were composited into equal lengths, such as 2, 3, or 5 meters. Sample lengths in this deposit ranged from approximately 0.2 meters to 7 meters, with an

average sampling interval of 1.6 meters of core length analyzed per sample. Of the total 3,988 meters drilled, approximately 2,908 meters were from boreholes and 1,079 meters from trenches, with about 2,626 meters sampled.

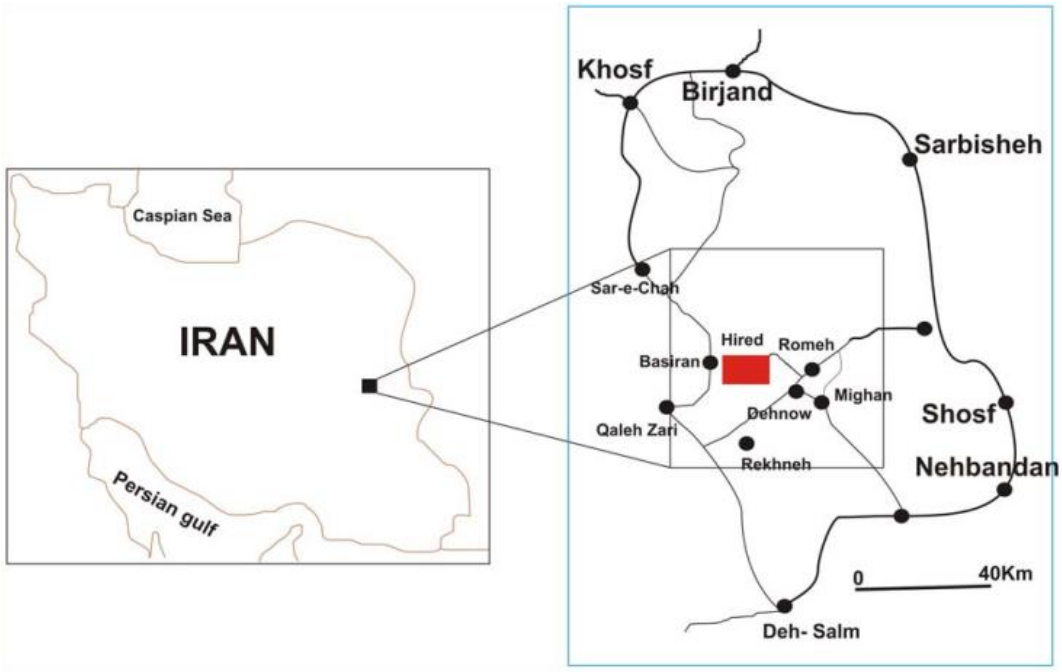

Fig. 1. Location map of Hired mineralization area (Haidarian Shahri et al. 2010)

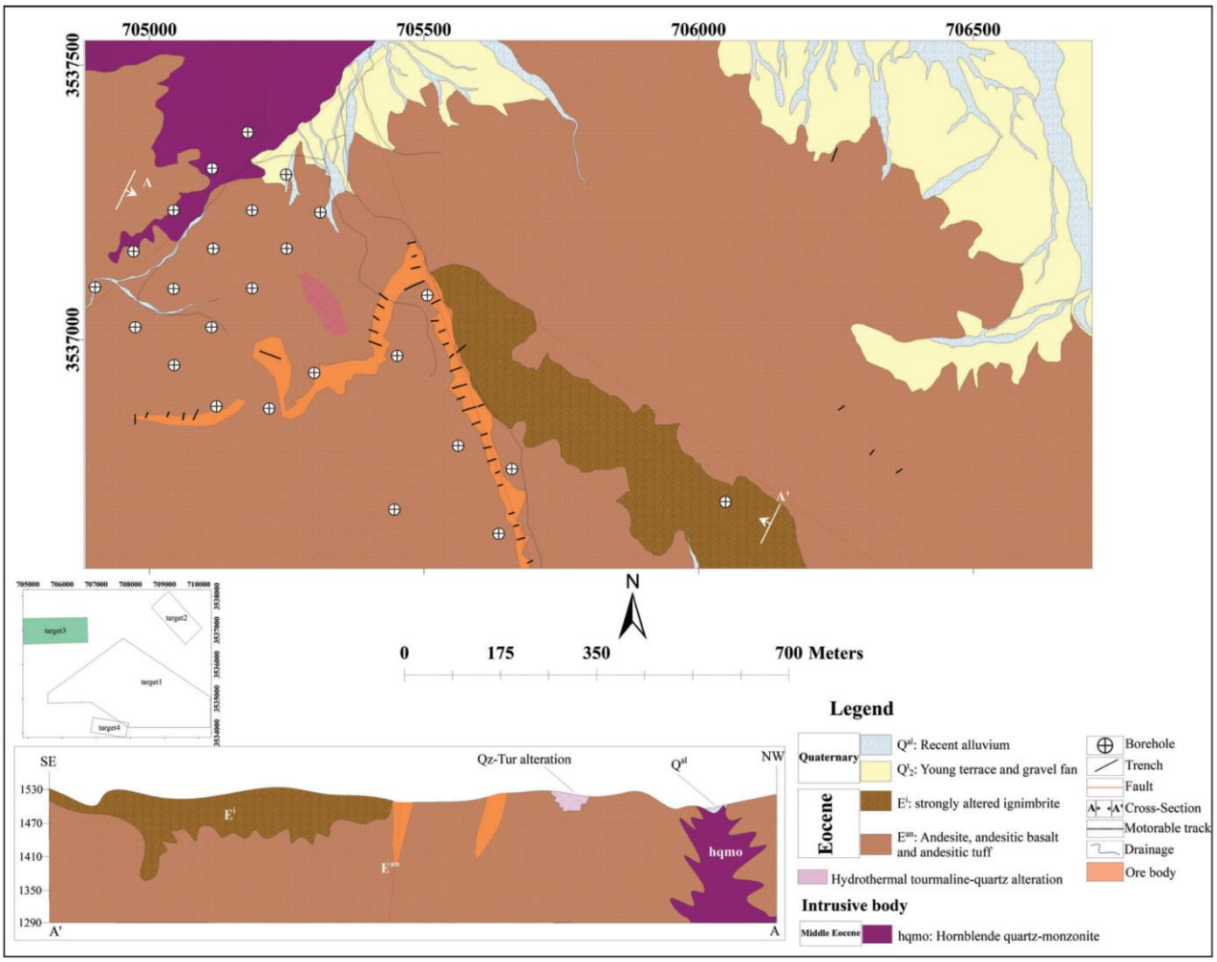

Fig. 2 Geological map of Anomaly No. 3, Heird gold deposit (Emami Jafari et al, 2023)

The collected samples represent a heterogeneous and non-equiprobable dataset, necessitating the conversion of all samples into composites of fixed lengths. In this study, Surpac and Datamine software were used for ordinary kriging and indicator kriging methods, respectively, while Isatis software was used for sequential Gaussian simulation (Fig. 3). A composite length of 1.5 meters was selected based on the average sampling interval of the collected borehole and trench data, which was approximately 1.6 meters. This length was chosen to minimize data loss and ensure consistency across different sampling sources. In addition, trial compositing with lengths of 2 m and 3 m was conducted; however, the 1.5 m composites provided the most balanced representation of grade continuity and statistical stability. This approach preserved the spatial resolution of the original dataset while maintaining an adequate number of data points for reliable geostatistical modeling. Based on these results, a total of 2,124 gold composites were generated using the 1.5-meter composite length. Table 1 presents the basic statistics of the composite data.

The statistical results, particularly the high skewness (13.66) and kurtosis (282.52) values, indicate a strongly non-normal distribution of gold grades. This pattern is typical of epithermal and vein-type gold deposits, where a small number of high-grade samples dominate the dataset. Such a positively skewed distribution significantly affects the performance of linear estimation techniques, such as Ordinary Kriging, which assume normality. Therefore, non-parametric methods—especially Full Indicator Kriging (FIK)—were employed in this study, as they are less sensitive to extreme values and provide more reliable estimates for highly skewed data.

According to the calculated parameters, the average grade of the composites is 0.45 ppm. The frequency distribution histogram of the composited gold grades closely resembles that of the raw data, with both exhibiting an L-shaped pattern. Given this L-shaped distribution, applying logarithmic transformations for normalization is recommended.

Table 1. Basic statistics of composite data

Parameter	Boreholes	Teranches	Total data
Number of Samples	1453	671	2124
Minimum Sample (ppm)	0.001	0.001	0.001
Maximum Sample (ppm)	29.7	48	48
Mean (ppm)	0.23	0.94	0.45
Variance (ppm^2)	1.51	6.76	3.29
Standard Deviation (ppm)	1.23	2.56	1.81
Coefficient of Variation	5.43	2.75	4.66
Skewness	15.08	10.72	13.66
Kurtosis	300.43	171.56	282.52

One challenge that can complicate geostatistical estimates is the presence of trends in the data. To address this, geometric tests should be conducted on the different variables to identify and remove any trends before performing the estimation. One of the simplest methods for detecting trends is to plot scatter diagrams of the grade in the north-south (Y), east-west (X), and depth (Z) directions. This approach helps identify any apparent trends in grade variations, ensuring that appropriate measures are taken to prevent these trends from influencing the estimates. Fig. 4 presents the scatter diagram of gold grades for samples within the estimation space along the X, Y, and Z direction, where no significant trend in grade variations is observed.

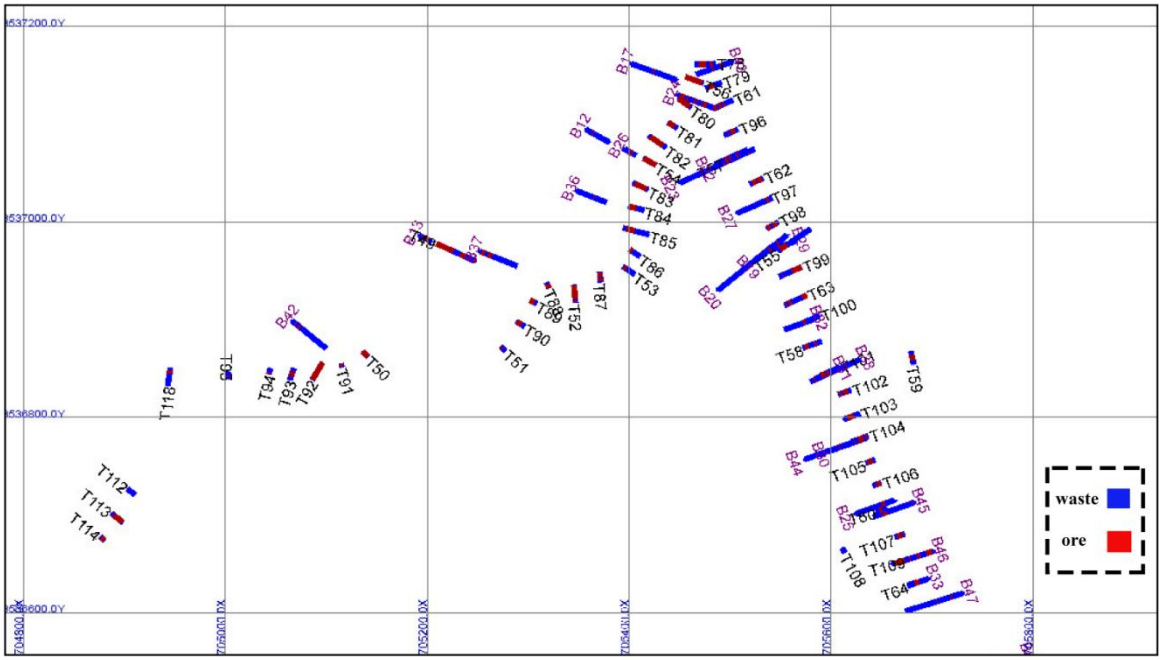

Fig. 3. 2D view of excavations at Hird Gold Anomaly 3

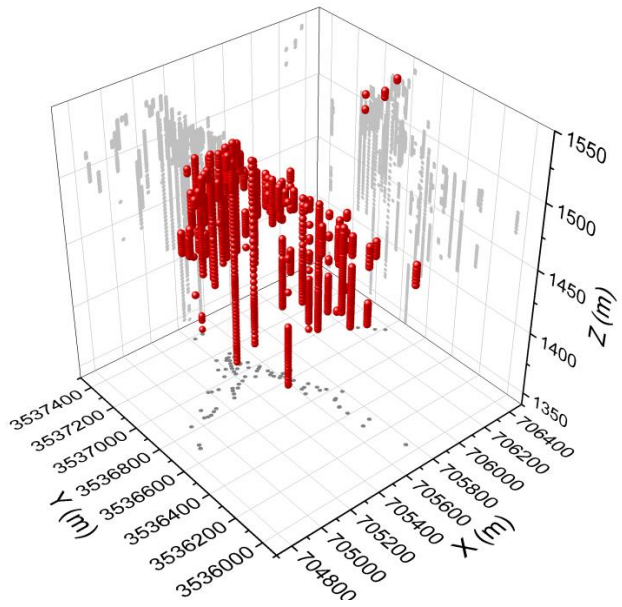

Fig. 4. Gold grade distribution and their projection on XY, XZ, and YZ

IV. METHODS AND ANALYSES

A. *Spatial Continuity and Variogram*

After normalizing the data using the z-score method, the experimental variogram of the normalized values was plotted alongside fitted spherical, power, and cubic models (Table 2 and Fig. 5). Examination of the variogram in different directions revealed no trend in spatial continuity. Consequently, an isotropic variogram was calculated for further analysis.

To validate the variogram, a graph comparing the observed and modeled values is presented in Fig. 6, demonstrating an 80% correlation. This 80% correlation represents the coefficient of determination (R^2) between the experimental and modeled variogram values. It indicates the degree of agreement between the observed spatial variability of the data and the fitted spherical model, confirming that the selected model provides a reliable representation of grade continuity for subsequent geostatistical estimation. Additionally, the histogram of the residuals exhibits an approximately normal distribution with no significant bias.

Table 2. Information on the change graph in three different models

Model	Cubic	Spherical	Power
Effect of Segment	0.59	0.53	0.40
Range	9.43	9.40	9.56
Threshold	0.10	0.10	0.11
Sum of Squared Residuals	0.000985	0.000927	0.000100

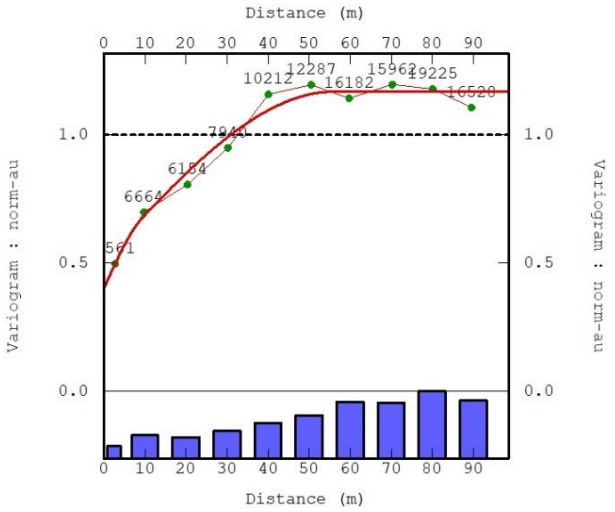

Fig. 5. Power variogram model

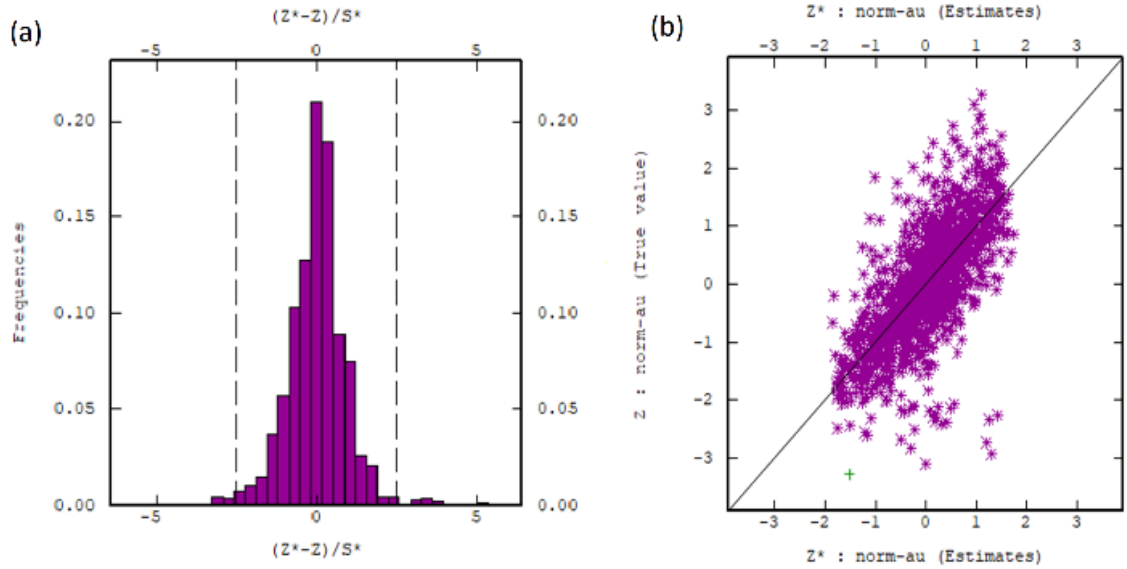

Fig. 6. (a) Error histogram (normal distribution); (b) Correlation diagram of estimated and actual data

B. Three-Dimensional Modeling of the Ore Body

Accurate estimation of the shape, position, size, and characteristics of the extractable ore body is essential for the technical and economic evaluation of the exploration project and the design of the extraction workshop. The accuracy and precision of the constructed geometric model depend on the type and quantity of available data. To create a three-dimensional model of the ore body, cross-sectional, longitudinal, and horizontal plans are prepared at regular intervals. The three-dimensional shape of the mineralized body is then obtained by linking these sections. In the next step, the three-dimensional body is filled with blocks of regular dimensions. In Fig. 7, the ore body boundary and the shape of the mineral distribution are initially plotted based on composited boreholes from previous stages. In subsequent stages, this boundary will be block-modeled, and estimation will be performed within these blocks. Fig. 7 shows the wireframe of the mineral body beneath the topographic surface.

C. Determination of the Estimation Space and Gridding of the Study Area

Constraining the estimation space minimizes the risks associated with averaging. To define this space, the continuity of ore and waste, as well as the structural orientation of mineralized veins based on existing evidence, were taken into account. The most critical factor controlling mineralization in this deposit is the host rock; in simple terms, mineralization has occurred within the limestone layers. The bottom of the orebody is defined by the deepest limestone layer intersected by the drill holes, while the top of the orebody corresponds to the surface topography. The resulting three-dimensional volume represents the domain within which the estimation must be carried out. Fig. 8 illustrates a three-dimensional view of the estimation space in Anomaly 3 of the Heird deposit. Accordingly, the estimation space encompasses the entire geometric model of the mineralized body. When designing a simulation grid, the grid origin, cell dimensions, number of cells in the three spatial directions, and the rotation angle relative to north must be specified. The minimum calculable lag is one of the key parameters used to define cell dimensions. Based on statistical and geostatistical analyses, the block dimensions were selected considering the following criteria:

Mode of orebody extension: If the mineralization extends isotropically, square blocks are recommended in plan view. However, even when anisotropy is present in the shape of the mineralized body, square blocks in plan view are still preferred.

D. Continuity of ore and waste: The vertical dimension of the blocks is influenced by the continuity of both ore and waste. Considering the relatively small thickness of the mineralized high-grade zone, the average sampling interval, and the large spacing between drill holes (minimum 45 m), block dimensions of 1 × 1 × 1 m were selected.

E. Ordinary Kriging

In this method, estimation is performed using the final raw data obtained from drilling and trenches. After analyzing the concepts of continuity, mineralization persistence, isotropy, and anisotropy in the region, as well as the spatial structure of the deposit through variography, the parameters of the search ellipse were calculated. Estimation was then conducted using ordinary kriging (Fig. 8).

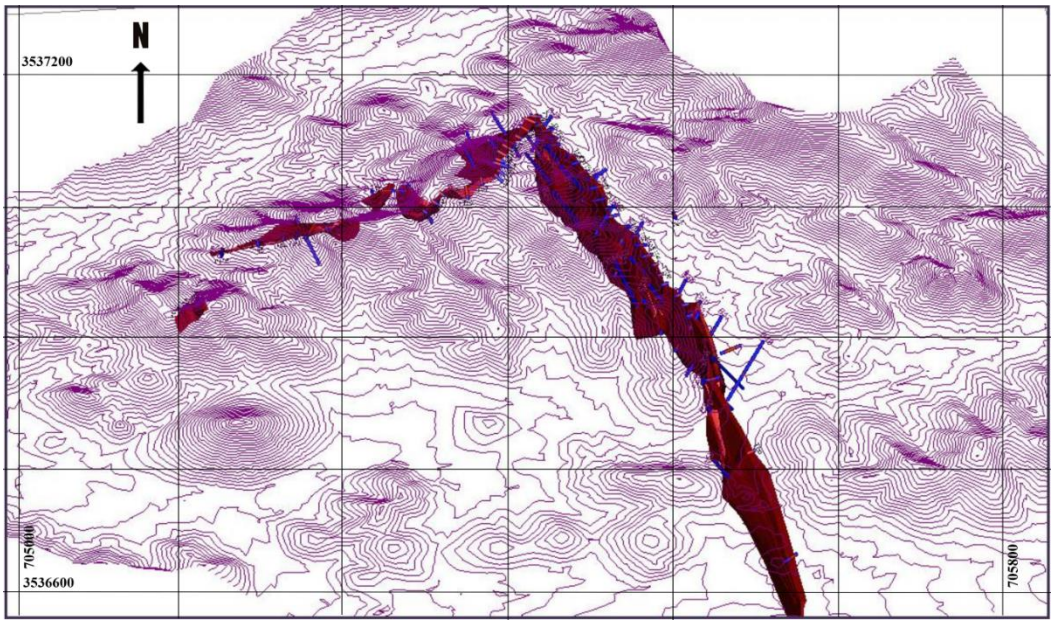

Fig. 7. Wireframe model of the mineralized body beneath the topographic surface

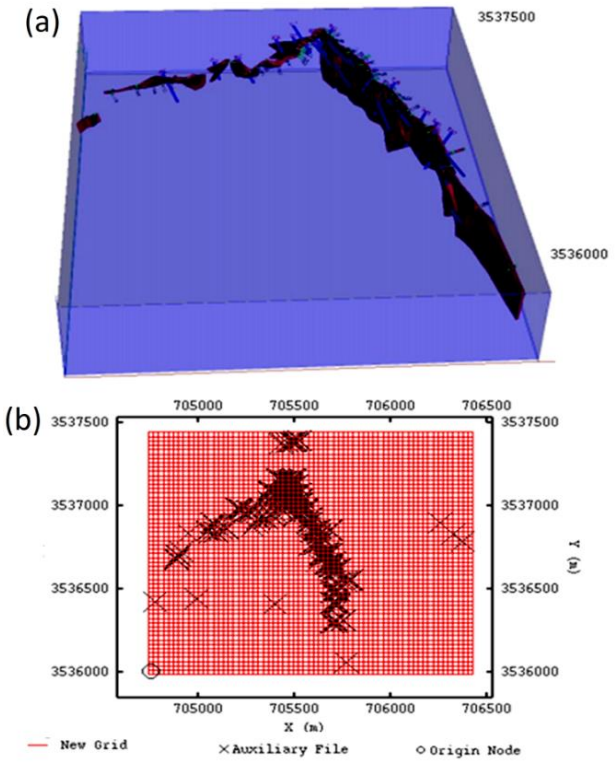

Fig. 8. (a) Constraining the study area; (b) Block modeling of the study area and definition of the grid origin coordinate.

F. Indicator Kriging

At this stage, the data were first converted into binary values (0 and 1). Values below the threshold of 0.1 were classified as waste, while values above this threshold were considered mineralized. Variography was then performed to examine the spatial continuity of the binary data. Fig. 9 shows the isotropic variogram for the observed 0-1 data. This model was fitted with various models (spherical, cubic, and power), and the best-fitting model with the lowest error was selected. Fig. 9 also shows the variogram for the indicator kriging data. Following the application of indicator kriging to the data, a three-dimensional simulation was performed (Fig. 10).

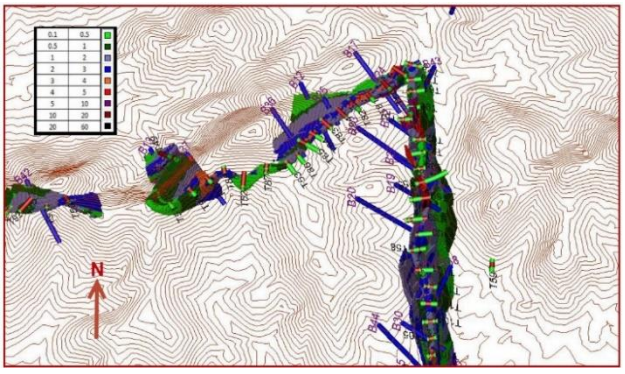

Fig. 8. 3D view of blocks estimated using ordinary kriging.

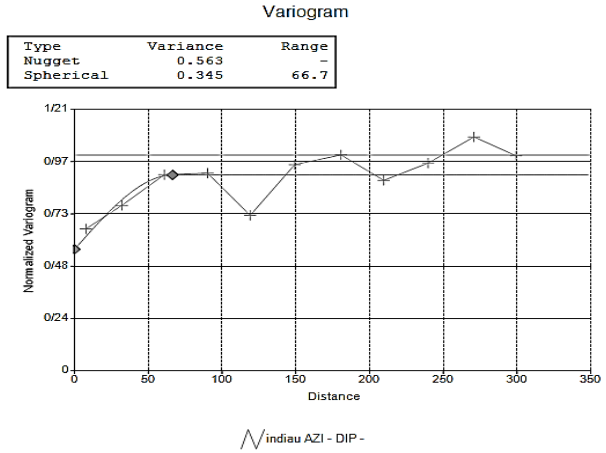

Fig. 9. Graph of change in the graph on the full index kriging data.

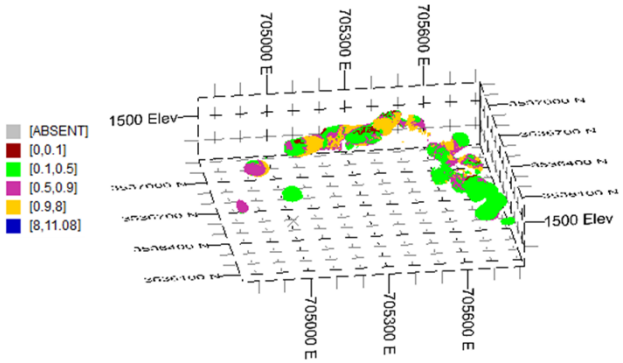

Fig. 10. Results from Kriging Estimation of the Index in Hird Gold Anomaly 3

- Sequential Gaussian Simulation

G. At this stage, sequential Gaussian simulation was conducted, and the results of 100 simulations were presented as 3D maps depicting various elevation levels. Expected value maps and cumulative distribution function (CDF) plots of the simulations were then prepared and analyzed. Finally, uncertainty maps and probability maps were generated (Fig. 11). After performing the estimation using the three methods mentioned, the results are summarized in Table 3.

H. Grade-Tonnage Curve

To summarize the results from the estimation methods, grade-tonnage curves were plotted and analyzed for each method used. As shown in the tables, the calculated total ore tonnage is as follows:

- 3,910,000 tons with an average grade of 0.92 g/t for ordinary kriging
- 3,420,000 tons with an average grade of 0.75 g/t for indicator kriging
- 3,560,000 tons with an average grade of 0.70 g/t for sequential Gaussian simulation

To select the best method and calculate the final ore reserve, cross-validation was conducted to identify the optimal approach.

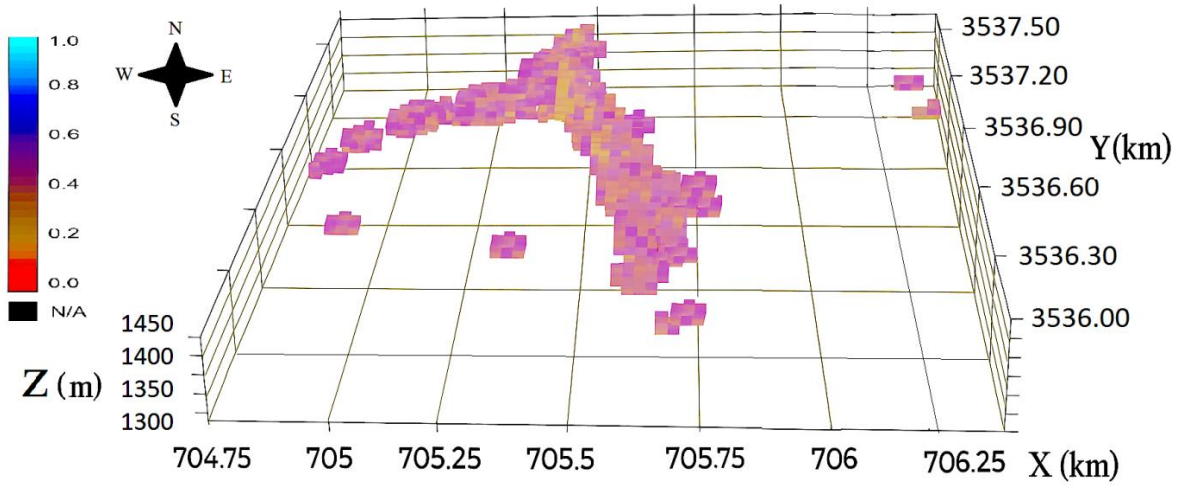

Fig. 11. The probability map of values greater than the threshold of 0.1

Table 3. Results of Estimation Using Ordinary Kriging, Indicator Kriging, and Sequential Gaussian Simulation

Cut-off Grade (ppm)	Gaussian Simulation		Indicator Kriging		Ordinary Kriging	
	Tonnage (Mt)	Avg. Grade (g/t)	Tonnage (Mt)	Avg. Grade (g/t)	Tonnage (Mt)	Avg. Grade (g/t)
0.1	3.56	0.70	3.42	0.75	3.91	0.92
.2	3.42	0.90	3.30	0.83	3.50	1.00
0.3	3.18	1.31	3.12	0.96	3.32	1.14
0.4	3.01	1.25	2.82	1.02	3.09	1.32
0.5	2.90	1.42	2.50	1.09	2.53	1.47
0.7	2.80	1.70	1.69	1.78	1.62	1.88
1.0	2.70	1.60	0.92	1.92	0.98	2.19
1.25	1.50	2.66	0.90	1.23	0.93	2.50
1.5	1.00	2.74	0.83	2.62	0.79	2.93
2.0	0.95	3.14	0.72	2.89	0.63	3.34
2.5	0.69	4.68	0.34	3.32	0.34	4.41
3.0	0.22	5.12	0.25	4.82	0.22	5.39
3.5	0.15	6.26	0.16	5.32	0.16	6.17
4.0	0.12	6.83	0.12	5.75	0.14	6.75
5.0	0.07	9.49	0.04	9.32	0.06	9.58
6.0	0.03	10.04	0.03	10.24	0.05	10.38

I. Cross-Validation

At this stage, cross-validation was performed using the entire actual dataset. The results are presented as scatter plots, with the method exhibiting the highest correlation coefficient considered the closest to the actual data. The validation results indicate that indicator kriging has a higher correlation coefficient than the other two methods (Fig.s 12, 13, and 14).

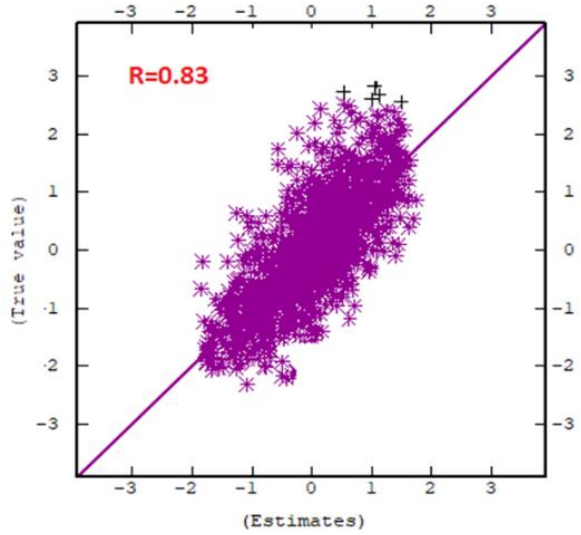

Fig. 12. The scatter plot for cross-validation using indicator kriging

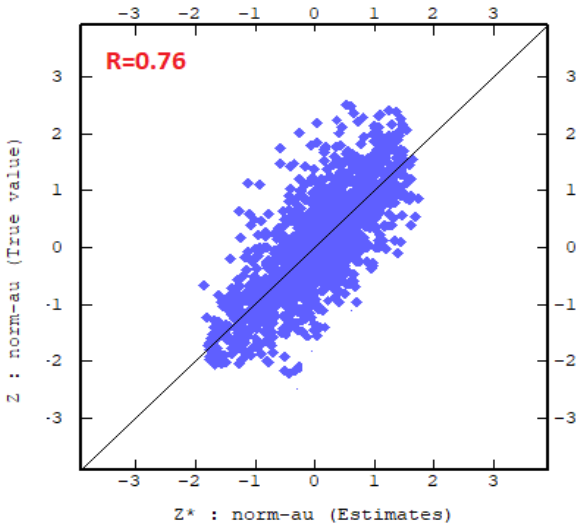

Fig. 13. The scatter plot for cross-validation using sequential Gaussian simulation

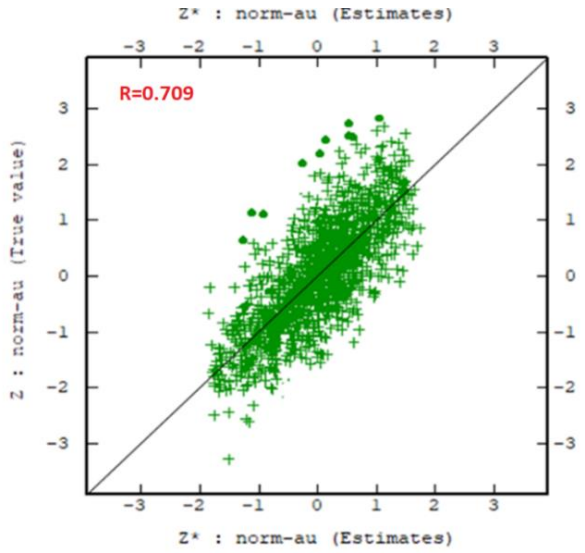

Fig. 14. The scatter plot for cross-validation using ordinary kriging

V. CONCLUSION

This study compared three geostatistical methods—Ordinary Kriging (OK), Full Indicator Kriging (FIK), and Sequential Gaussian Simulation (SGS)—for estimating the reserves of the Hired gold deposit (Anomaly 3). The results demonstrate that while OK produced higher average grades and SGS provided useful uncertainty maps, FIK offered the most consistent estimates aligned with the actual grade distribution. Quantitative validation using grade–tonnage curves, cross-validation statistics, and error metrics confirmed that FIK minimized the influence of extreme high-grade values and more accurately represented the variability of gold mineralization. At a cut-off grade of 0.1 g/t, FIK estimated 3.42 Mt of ore with an average grade of 0.75 g/t.

The study is subject to certain limitations, including relatively sparse drilling in parts of the deposit and potential structural complexities that may not be fully captured by the applied models. Therefore, future work should include additional drilling, integration of geological and structural modeling, and the application of advanced simulation techniques to improve the robustness of resource classification.

Overall, this research highlights the suitability of FIK for deposits with highly skewed grade distributions, particularly in gold systems, and provides a methodological framework that can facilitate more reliable resource estimation and mine planning.

REFERENCES

Abzalov, M., & Humphreys, M. (2002). Resource estimation of structurally complex and discontinuous mineralization using non-linear geostatistics: Case study of a mesothermal gold deposit in Northern Canada. Exploration and Mining Geology, 11(1–4), 19–29.

Adhikary, P. P., Dash, C. J., Bej, R., & Chandrasekharan, H. (2011). Indicator and probability kriging methods for delineating Cu, Fe, and Mn contamination in groundwater of Najafgarh Block, Delhi, India. Environmental Monitoring and Assessment, 176(1–4), 663–676.

Al-Hassan, S., & Boamah, E. (2015). Comparison of ordinary kriging and multiple indicator kriging estimates of Asuadai deposit at Adansi Gold Ghana Limited. Ghana Mining Journal, 15(2), 42–49.

Aghanabati, S. A. (2013). Geology of Iran and Neighbouring countries. Geological Survey of Iran.

Antunes, I., & Albuquerque, M. (2013). Using indicator kriging for the evaluation of arsenic potential contamination in an abandoned mining area (Portugal). Science of the Total Environment, 442, 545–552.

Askari, A., Karimpour, M. H., Mazaheri, S. A., & Malekzadeh, A. (2015). Interpretation of Geophysical Survey (IP/RS) in Hired Gold Prospecting Area Using Geology, Alteration and Mineralization Data.

Aryafar, A., & Moeini, H. (2017). Application of continuous restricted Boltzmann machine to detect multivariate anomalies from stream sediment geochemical data, Korit, East of Iran. Journal of Mining and Environment, 8(4), 673-682.

Aryafar, A., Moeini, H., & Khosravi, V. (2020). CRFA-CRBM: a hybrid technique for anomaly recognition in regional geochemical exploration; case study: Dehsalm area, east of Iran. International Journal of Mining and Geo-Engineering, 54(1), 33-38.

Aryafar, A., & Roshanravan, B. (2020). Improved index overlay mineral potential modeling in brown-and green-fields exploration using geochemical, geological and remote sensing data. Earth Science Informatics, 13(4), 1275-1291.

Aryafar, A., & Roshanravan, B. (2021). BWM-SAW: A new hybrid MCDM technique for modeling of chromite potential in the Birjand district, east of Iran. Journal of Geochemical Exploration, 231, 106876.

Badel, M., Angorani, S., & Panahi, M. S. (2011). Application of median indicator kriging and neural network in modeling mixed population in an iron ore deposit. Computers & Geosciences, 37(4), 530–540.

Chanderman, L., Dohm, C. E., & Minnitt, R. C. A. (2017). 3D geological modelling and resource estimation for a gold deposit in Mali. Journal of the Southern African Institute of Mining and Metallurgy, 117(2), 189–197.

Daya, A.A. (2012). Reserve estimation of central part of Choghart north anomaly iron ore deposit through ordinary kriging method. International Journal of Mining Science and Technology, 22 (4), 573-577.

Daya, A.A., Zaremotlagh, S (2013). A comparative analysis between disjunctive kriging and ordinary kriging for estimating the reserve of a mine: A case study of Choghart iron ore deposit. J of Min Met 49 (1), 1-8.

Daya, A.A. (2014). Application of disjunctive kriging for estimating economic grade distribution in an iron ore deposit: A case study of the Choghart North Anomaly, Iran. Journal of the Geological Society of India 83 (5), 567-576.

Daya, A.A. (2015). Application of median indicator kriging in the analysis of an iron mineralization. Arabian journal of Geosciences 8 (1), 367-377.

Dehshibi, R., Karami, S., Maleki, Z., & Farhadian, H. (2022). A comparative study on evaluation of steady-state groundwater quality in Sirjan's Golgohar mineral zone. Arabian Journal of Geosciences, 15(9), 842.

Dominy, S. C., Noppé, M. A., & Annels, A. E. (2002). Errors and uncertainty in mineral resource and ore reserve estimation: The importance of getting it right. Exploration and Mining Geology, 11, 77–98.

Emami Jafari, M., Alirezaei, S., Rasa, I., & Kolb, J. (2023). The Hired gold deposit, Lut Block, East Iran: example of a gold deposit related to reduced I-type intrusive bodies. Scientific Quarterly Journal of Geosciences, 33(3), 219-242.

Farhadian, H. (2021). A new empirical chart for rockburst analysis in tunnelling: Tunnel rockburst classification (TRC). International Journal of Mining Science and Technology, 31(4), 603-610.

Farhadian, H., & Dehshibi, R. (2025). Geostatistical Analysis of Groundwater Levels at Tangab Dam Using IDW, Kriging, and Sequential Gaussian Simulation. Journal of Hydraulic Structures, 167-187.

Farhadian, H., & Maleki, Z. (2023). Groutability classification of granular soils with cement grouts. Journal of Rock Mechanics and Geotechnical Engineering, 15(6), 1580-1590.

Farhadian, H., & Nikvar-Hassani, A. (2020). Development of a new empirical method for Tunnel Squeezing Classification (TSC). Quarterly Journal of Engineering Geology and Hydrogeology, 53(4), 655-660.

Ghahremani, L. (2017). Remodeling and resource estimation of Golegohar Iron Ore Mine No. 2 using ordinary kriging and sequential Gaussian simulation (Master's thesis). Shahid Bahonar University of Kerman.

Goovaerts, P. (1997). Geostatistics for natural resources evaluation. New York: Oxford University Press.

Goovaerts, P. (2009). AUTO-IK: A 2D indicator kriging program for the automated non-parametric modeling of local uncertainty in earth sciences. Computers & Geosciences, 35(6), 1255–1270.

Haidarian Shahri, M. R., Karimpour, M. H., & Malekzadeh, A. (2010). The exploration of gold by magnetic method in Hired Area, South Khorasan, a case study. Journal of the Earth & Space Physics, 35(4), 33-44.

Hasani Pak, A. H., & Sharafedin, M. (2001). Exploratory data analysis. Tehran: University of Tehran Press.

Journel, A. G. (1986). Geostatistics: Models and tools for the earth sciences. Mathematical Geology, 18(1), 119–140.

Kapageridis, I. K. (1999). Application of artificial neural network systems to grade estimation from exploration data (Doctoral dissertation). University of Nottingham.

Kyriakidis, P. C., & Journel, A. G. (1999). Geostatistical space–time models: A review. Mathematical Geology, 31(6), 651–684.

Lin, Y. P., Chang, T. K., Shih, C. W., & Tseng, C. H. (2002). Factorial and indicator kriging methods using a geographic information system to delineate spatial variation and pollution sources of soil heavy metals. Environmental Geology, 42, 900–909.

Lloyd, C., & Atkinson, P. M. (2001). Assessing uncertainty in estimates with ordinary and indicator kriging. Computers & Geosciences, 27(8), 929–937.

Nejad Hosseini Fashkhami, H. (2009). 3D modeling and estimation of Kuhnech Eastern Cu-Mo anomaly using geochemical, geophysical, and exploratory borehole data (Master's thesis). Isfahan University of Technology.

Parker, H. M. (1991). Statistical treatment of outlier data in epithermal gold deposit reserve estimation. Mathematical Geology, 23(2), 175–199.

Rahimi, H. (2016). Modeling and resource estimation of Qolqoleh gold deposit (SW Saqqez) using ordinary, indicator, and probability kriging methods (Master's thesis). Urmia University.

Rahimi, H., Asghari, O., Hajizadeh, F., & Meysami, F. (2016). Assessment the number of thresholds on tonnage-grade curve in IK estimation: Case study: Qolqoleh gold deposit (NW of Iran).

Rossi, M. E., & Deutsch, C. V. (2013). Mineral resource estimation. Springer Science & Business Media.

Rostamipour, H., Behzadi, M., Movahedi, M., & Amini, M. (2024). Mineralization of gold, copper and associated metals in the northern Hired area, South Khorasan, East Iran. Researches in Earth Sciences/Pizhūhish/hā-yi Dānish-i Zamīn, 15(2).

Saed, S., & Farhadian, H. (2025). A survey on spatial variations of groundwater quality in Kabul, Afghanistan and its evaluation for different uses. Journal of Irrigation Sciences and Engineering 4(47): 17-34.

Saito, H., & Goovaerts, P. (2000). Geostatistical interpolation of positively skewed and censored data in a dioxin-contaminated site. Environmental Science & Technology, 34(19), 4228–4235.

Samani, B., & Ashtari, M. (1992). Geological Development of the Sistan and Baluchestan Region. Journal of Earth Sciences, 1(4), 25-14.

Shademan, M., & Farhadian, H. (2023). Contribution of geostatistical modeling on simulating a geomechanical parameter (case study: GSI in Gol-Gohar open pit iron mine, Kerman, southeastern Iran). Journal of Geomine, 1(2), 81-91.